Free-molecule heat transfer in a conservative force field between parallel surfaces

Steffen Hardt*

Institute for Nano- and Microfluidics, Center of Smart Interfaces, Technische Universität Darmstadt, Germany

(Received 4 January 2016; revised manuscript received 8 March 2016; published 20 May 2016)

The heat flux between parallel surfaces is computed analytically assuming that heat is transferred by particles moving ballistically under the influence of a conservative force field. Particle reflection at the surfaces is governed by a Maxwell-type boundary condition. It is found that the force field can give rise to a substantial reduction, but also to an enhancement of the heat flux, depending on the ratio of the temperatures at the two surfaces. The influence of the accommodation coefficients is studied. An asymmetry introduced by the force field and/or the boundary conditions at the two surfaces causes a significant heat-flux rectification, characteristic for a thermal diode.

DOI: 10.1103/PhysRevE.93.052139

I. INTRODUCTION

Heat may be transferred by atoms or molecules in a fluid, or by electrons or phonons in a solid. In the regime where the wavelike character of these entities does not play a role, they can be modeled as classical particles. Within certain limits, the kinetics of these particles is described by the Boltzmann equation, most notably when their number density is low enough to describe particle-particle interactions as pointlike and to exclusively consider binary collisions. The Boltzmann equation has been established as a standard description for particle transport away from thermodynamic equilibrium in a number of different contexts. First of all, it is used to model gas dynamics in the rarefied regime [1,2]. It has also found widespread applications in modeling electron transport in semiconductors in the semiclassical domain [3,4]. Even phonon transport in solids is often described based on the Boltzmann equation [5,6].

The most important dimensionless group characterizing these transport processes is the Knudsen number Kn, being the ratio between the mean free path of the particles and a characteristic system dimension. For $\mathrm{Kn} \gg 1$, the collisions between particles can be neglected, and transport phenomena can be analyzed based on ballistic particle trajectories. In gas kinetics, this is referred to as the free-molecular flow regime. A classical result in that context is the free-molecular heat flux between two parallel surfaces with complete thermal accommodation (see, e.g., [7]):

$$q_{\mathrm{fm}} = \frac{\rho}{\sqrt{\pi}}(2R)^{3/2}\sqrt{T_1 T_2}(\sqrt{T_1} - \sqrt{T_2}). \tag{1}$$

In this expression, T_1 and T_2 are the surface temperatures, ρ is the mass density of the particles, and R is the specific gas constant.

There are various situations in which ballistic heat transport becomes important. For example, apart from the classical case of a rarefied gas confined between two surfaces, ballistic transport also plays a role for the electronic contribution to solid heat transfer on the nanoscale. Solid structures with a characteristic scale below 100 nm in at least one dimension play a key role in a plethora of scientific and technological settings, and the mean free path of electrons at room temperature can be of the order of 50 nm [8,9]. Several extensions and generalizations of the relationship shown in Eq. (1) have been presented in the literature. First, Eq. (1) was generalized to account for a broader class of boundary conditions at the two surfaces [10]. Further, using numerical schemes for solving the kinetic equations, the effects of particle-particle collisions on heat transfer between parallel surfaces have been studied [11–17].

Among others, nanoscale heat transport plays a key role in current efforts to design thermoelectric devices with increased efficiency [18,19]. Thermoelectric energy converters often utilize nanostructures with characteristic dimensions comparable to the mean free path of electrons and phonons, and are based on the idea of increasing the ratio of electric and thermal conductivity compared to the value characteristic for bulk materials. Motivated by this example, it appears as if one important aspect of ballistic heat transfer between parallel surfaces has not been considered up to now: Close to the surface of a solid (or close to the interface to a second phase or material), electrons or phonons may experience a mean force field. For example, in metals the corresponding effective potential is related to the work function and increases when an electron approaches the surface [20]. Similarly, ions moving in an electric field applied between two surfaces experience an electrostatic potential.

While the examples above may appear a bit exotic, heat transfer by ballistic particle transport in a mean force field between two parallel surfaces is a quite ubiquitous phenomenon also within the quite classical scope of a gas confined in a gap at high Knudsen numbers. The following order-of-magnitude arguments suggest that neglecting the mean force field onto atoms or molecules in a gas [as inherent in Eq. (1)] is usually not supported by the physics of gas-surface interactions.

Atoms or molecules in a gas interact with a surface via van der Waals forces. Based on an interaction potential between two atoms or molecules of the form $U_{\mathrm{aa}} = -C/r^6$ (r: separation distance), a simplified expression for the interaction potential between an atom or molecule and a planar wall is given as [21]

$$U_{\mathrm{as}} = -\frac{\pi}{6}\frac{Cn}{d^3}, \tag{2}$$

where d is the distance between an atom or molecule and the surface, and n is the number density of atoms or molecules in the wall material. For simplicity, is has been assumed that

*hardt@csi.tu-darmstadt.de

the atoms or molecules in the gas and in the wall material are identical. Let us consider the interaction of argon with a surface. From the Lennard-Jones parameters of argon (see, e.g., [22,23]) we obtain $C \approx 1.1 \times 10^{-77}\,\mathrm{J\,m^6}$. In order to transfer energy to a surface of an electrically insulating material, an atom has to collide with surface atoms or molecules and excite or destroy phonons. Generally, this is a complex problem requiring a quantum mechanical treatment (see [24] and references therein). However, in a simple classical picture we can assume that energy transfer between an atom and a surface only happens when there is a geometric overlap between the surface structures and the atom. The corresponding geometric quantity enabling mapping the electron cloud of argon to a sphere is the van der Waals radius r_W. For argon we have $r_\mathrm{W} \approx 0.188\,\mathrm{nm}$ [25]. Correspondingly, at the point of contact of an argon atom with a flat surface at $T = 300\,\mathrm{K}$, Eq. (2) gives $U_\mathrm{as} \approx -12.7 k_\mathrm{B} T$, where k_B is the Boltzmann constant, and a characteristic value of $n = 10^5\,\mathrm{mol\,m^{-3}}$ was assumed. This potential energy value is a manifestation of the fact that atoms or molecules can be adsorbed at surfaces. Generally, the magnitude of this value depends on the combination of wall material and gas species. This picture suggests that before atoms or molecules transfer energy to a surface, they are often exposed to an attractive van der Waals potential of significant magnitude. When considering the ballistic flight of gas atoms or molecules between two parallel surfaces, owing to the material dependence of van der Waals interactions, the effects of the attractive potentials at the two surfaces generally do not cancel each other, and the fact that the atoms or molecules are exposed to a force field needs to be taken into account.

The examples above motivate developing a theory for free-molecule heat transfer between parallel surfaces in a conservative force field. For this purpose, it is assumed that the heat is carried by "particles," a generic term representing entities such as atoms, molecules, ions, electrons, or phonons, depending on the situation considered.

II. CALCULATION OF HEAT FLUX

Particle transport is modeled based on the collisionless Boltzmann equation,

$$\frac{\partial f}{\partial t} + \mathbf{c} \cdot \nabla_\mathbf{r} f + \frac{\mathbf{F}}{m} \cdot \nabla_\mathbf{c} f = 0, \tag{3}$$

where $f(\mathbf{r},\mathbf{c},t)$ is the phase-space distribution function of the particles (defined on the product space of position and velocity), m the particle mass, and $\mathbf{F}$ the force field. A conservative force field derived from a potential via $\mathbf{F} = -\nabla U$ is assumed. In the absence of collisions between particles, the Boltzmann equation can be solved by computing ballistic particle trajectories [2]. Figure 1 depicts the specific situation considered in this article. Particles move ballistically between two infinitely extended parallel surfaces. The lower surface (1) has a temperature of T_1, the upper one (2) a temperature of T_2. It is assumed that the two surfaces are isosurfaces of the potential energy. Without loss of generality, we specify $U = 0$ at the lower surface and $U = U_\mathrm{s} \geqslant 0$ at the upper surface. For solving the collisionless Boltzmann equation and computing the heat flux, boundary conditions at the two surfaces need to de defined. We consider the commonly used Maxwell boundary

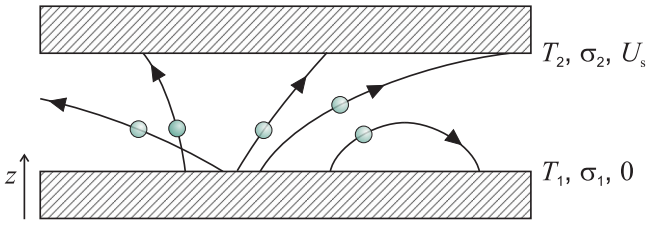

FIG. 1. Schematic showing particles moving ballistically between two surfaces. The parameters defining the boundary conditions are indicated.

condition, reading

$$f_\mathrm{out}(\mathbf{c}) = \sigma\, f_\mathrm{M}(\mathbf{c}) + (1-\sigma)\, f_\mathrm{in}(\mathbf{c}^*), \tag{4}$$

where f_out represents the phase-space distribution of the particles reflected from the corresponding surface, f_in that of the incoming particles, and f_M the Maxwell distribution, given by

$$f_\mathrm{M}(\mathbf{c}) = n\left(\frac{\beta m}{2\pi}\right)^{3/2} \exp\left(-\frac{1}{2}\beta m c^2\right), \tag{5}$$

with n being the particle number density and $\beta = (k_\mathrm{B} T)^{-1}$ (k_B: Boltzmann constant). The "*" superscript indicates inversion of the z component of velocity, i.e., $\mathbf{c}^* = (c_x, c_y, -c_z)$. σ is a momentum accommodation coefficient, being 1 for a diffusely reflecting surface and 0 for a surface with specular reflection. Different values σ_1, σ_2 are assumed for surfaces 1 and 2.

Figure 1 shows different trajectories of particles emerging from surface 1. By contrast to the situation without force field, not all of these particles reach surface 2. Some of them are directed back to surface 1 without transferring any energy.

To compute the heat flux between the surfaces, it is sufficient to know the phase-space distribution function at one of the surfaces. A steady-state solution is assumed. The key to the following analysis is to divide the velocity space into two subspaces, using the threshold velocity $c_\mathrm{t} = \sqrt{2U_\mathrm{s}/m}$. Considering energy conservation in the conservative force field, it follows that a particle emitted from surface 1 is only able to reach surface 2 if $c_z|_1 \geqslant c_\mathrm{t}$, where the subscript indicates at which velocity the surface is evaluated. Conversely, particles emitted from surface 2 reach surface 1 with $|c_z|_1 \geqslant c_\mathrm{t}$. In other words, all particles impinging on surface 1 with $|c_z|_1 < c_\mathrm{t}$ originate from surface 1 and have been redirected to this surface; all particles impinging with $|c_z|_1 \geqslant c_\mathrm{t}$ must have reached surface 2 before. Specifically, this means that for $|c_z|_1 < c_\mathrm{t}$ and when replacing c_z by $-c_z$, the phase-space distributions of the incoming and outgoing particles at surface 1 must be identical. At surface 1 we have

$$f_\mathrm{in}^{(1)}(\mathbf{c}^*) = \begin{cases} f_\mathrm{out}^{(1)}(\mathbf{c}) & \text{if } |c_z| < c_\mathrm{t} \\ N_- f_\mathrm{out}^{(2)}(\mathbf{c}^*_-) & \text{if } |c_z| \geqslant c_\mathrm{t} \end{cases}, \tag{6}$$

where the subscripts "in" and "out" refer to $c_z \leqslant 0$ ($c_z \geqslant 0$) and $c_z > 0$ ($c_z < 0$) for surface 1 (surface 2), respectively. The superscript indicates at which surface f should be evaluated. For particles impinging on surface 1 originating from surface 2 it needs to be taken into account that the z velocity increases during their ballistic flight. A velocity vector $\mathbf{c} = (c_x, c_y, c_z)$ at

surface 1 is therefore mapped to a velocity

$$\mathbf{c}_- = \left[c_x, c_y, c_z\sqrt{1 - 2U_s/\left(mc_z^2\right)}\right] \tag{7}$$

at surface 2. Correspondingly, to ensure particle number conservation, a normalization factor

$$N_- = \left(1 - \frac{2U_s}{mc_z^2}\right)^{-1/2} \tag{8}$$

has to be introduced. At surface 2, all of the incoming particles originate from surface 1. Correspondingly,

$$f_{\text{in}}^{(2)}(\mathbf{c}) = N_+ f_{\text{out}}^{(1)}(\mathbf{c}_+), \tag{9}$$

where $\mathbf{c}_+$ and N_+ are obtained by replacing the "–" signs under the square root in Eqs. (7) and (8) by "+" signs.

In what follows, a route toward computing $f_{\text{in}}^{(1)}$ and $f_{\text{out}}^{(1)}$ will be described. If $|c_z|_1 < c_t$, Eqs. (4) and (6) constitute a system of two equations for the two unknowns. If $|c_z|_1 \geqslant c_t$, Eq. (6) contains $f_{\text{out}}^{(2)}$ which can be reexpressed with the help of Eq. (4). Using Eq. (9) then again yields a closed system of equations for $f_{\text{in}}^{(1)}$ and $f_{\text{out}}^{(1)}$. As a result, we obtain

$$\begin{aligned} f_{\text{out}}^{(1)}(\mathbf{c}) &= \sigma_1 f_{\text{M}}^{(1)}(\mathbf{c}) + (1-\sigma_1) f_{\text{in}}^{(1)}\left(\mathbf{c}^*\right), \\ f_{\text{in}}^{(1)}\left(\mathbf{c}^*\right) &= f_{\text{out}}^{(1)}(\mathbf{c}), \end{aligned} \tag{10}$$

if $|c_z|_1 < c_t$ and

$$\begin{aligned} f_{\text{out}}^{(1)}(\mathbf{c}) &= \sigma_1 f_{\text{M}}^{(1)}(\mathbf{c}) + (1-\sigma_1) f_{\text{in}}^{(1)}(\mathbf{c}^*), \\ f_{\text{in}}^{(1)}\left(\mathbf{c}^*\right) &= \sigma_2 f_{\text{M}}^{(2)}\left(\mathbf{c}^*\right) + (1-\sigma_2) f_{\text{out}}^{(1)}(\mathbf{c}), \end{aligned} \tag{11}$$

if $|c_z|_1 \geqslant c_t$. The solution is

$$\begin{aligned} f_{\text{out}}^{(1)}(\mathbf{c}) &= f_{\text{M}}^{(1)}(\mathbf{c}), \\ f_{\text{in}}^{(1)}\left(\mathbf{c}^*\right) &= f_{\text{M}}^{(1)}(\mathbf{c}), \end{aligned} \tag{12}$$

if $|c_z|_1 < c_t$ and

$$\begin{aligned} f_{\text{out}}^{(1)}(\mathbf{c}) &= \frac{\sigma_1 f_{\text{M}}^{(1)}(\mathbf{c}) + (1-\sigma_1)\sigma_2 f_{\text{M}}^{(2)}(\mathbf{c})}{1-(1-\sigma_1)(1-\sigma_2)}, \\ f_{\text{in}}^{(1)}\left(\mathbf{c}^*\right) &= \frac{\sigma_2 f_{\text{M}}^{(2)}(\mathbf{c}) + (1-\sigma_2)\sigma_1 f_{\text{M}}^{(1)}(\mathbf{c})}{1-(1-\sigma_1)(1-\sigma_2)}, \end{aligned} \tag{13}$$

if $|c_z|_1 \geqslant c_t$. Via $f_{\text{M}}^{(1)}$ and $f_{\text{M}}^{(2)}$, this solution depends on the yet undetermined parameters n_1 and n_2.

To fix n_1 and n_2, we employ the following two conditions:

(1) The particle number density at surface 1 is given by n;

(2) The incoming particle number flux at surface 1 is equal to the outgoing particle number flux.

Since surface 1 has been chosen to determine n_1 and n_2, in the following we skip the superscripts at the phase-space distribution functions, adopting the convention that from this point on all phase-space distributions are evaluated at surface 1 if not stated otherwise. The first of the above two conditions is expressed as

$$\int_{c_z\leqslant 0} f_{\text{in}} d^3c + \int_{c_z>0} f_{\text{out}} d^3c = n. \tag{14}$$

After expressing f_{in} and f_{out} via Eqs. (12) and (13), splitting the velocity space into subspaces $S_- = \{\mathbf{c} \in \mathbb{R}^3 : |c_z| < c_t\}$ and $S_+ = \{\mathbf{c} \in \mathbb{R}^3 : |c_z| \geqslant c_t\}$, and performing the integrals over the two subspaces separately, Eq. (14) transforms into

$$\begin{aligned} n = \frac{n_1}{2}\left[2\text{erf}(\tilde{c}_{t1}) + \frac{\sigma_1(2-\sigma_2)[1-\text{erf}(\tilde{c}_{t1})]}{1-(1-\sigma_1)(1-\sigma_2)}\right] \\ + \frac{n_2}{2}\frac{\sigma_2(2-\sigma_1)[1-\text{erf}(\tilde{c}_{t2})]}{1-(1-\sigma_1)(1-\sigma_2)}, \end{aligned} \tag{15}$$

where erf is the error function and $\tilde{c}_{ti} = \sqrt{m\beta_i/2}\, c_t$. The condition of equal incoming and outgoing particle fluxes reads

$$\int_{c_z\leqslant 0} c_z f_{\text{in}} d^3c + \int_{c_z>0} c_z f_{\text{out}} d^3c = 0. \tag{16}$$

Again, the corresponding integrals can be evaluated in a straightforward manner, resulting in

$$n_2 = \sqrt{\frac{\beta_2}{\beta_1}}\exp\left(\tilde{c}_{t2}^2 - \tilde{c}_{t1}^2\right) n_1. \tag{17}$$

Equations (15) and (17) represent two equations for the two unknowns n_1 and n_2. The solution is

$$\begin{aligned} n_1 = 2n\Bigg(2\text{erf}(\tilde{c}_{t1}) + [1-(1-\sigma_1)(1-\sigma_2)]^{-1} \\ \times\Bigg\{\sigma_1(2-\sigma_2)[1-\text{erf}(\tilde{c}_{t1})] \\ + \sqrt{\frac{\beta_2}{\beta_1}}\exp\left(c_{t2}^2 - c_{t1}^2\right)\sigma_2(2-\sigma_1)[1-\text{erf}(\tilde{c}_{t2})]\Bigg\}\Bigg)^{-1}, \end{aligned} \tag{18}$$

together with Eq. (17).

For computing the heat flux between the two surfaces, it is assumed that the internal degrees of freedom of the particles (if any) remain unaffected by the collisions with the surfaces. Consequently, only the energy stored in the center of mass motion contributes, and the heat flux is given by

$$q = \frac{m}{2}\left(\int_{c_z\leqslant 0} c_z c^2 f_{\text{in}} d^3c + \int_{c_z>0} c_z c^2 f_{\text{out}} d^3c\right). \tag{19}$$

Again, by utilizing Eqs. (12) and (13), and by splitting the velocity space into two integration domains S_- and S_+, all integrals contributing to Eq. (19) can be evaluated in a straightforward manner, yielding

$$\begin{aligned} q = \sqrt{\frac{2}{\pi m}}\frac{\sigma_1\sigma_2}{1-(1-\sigma_1)(1-\sigma_2)}\Bigg[\frac{n_1}{\beta_1^{3/2}}\exp\left(-\tilde{c}_{t1}^2\right)\left(1+\tfrac{1}{2}\tilde{c}_{t1}^2\right) \\ - \frac{n_2}{\beta_2^{3/2}}\exp\left(-\tilde{c}_{t2}^2\right)\left(1+\tfrac{1}{2}\tilde{c}_{t2}^2\right)\Bigg] \end{aligned} \tag{20}$$

where n_1 and n_2 are given by Eqs. (17) and (18), respectively. For later convenience, it is preferable to introduce a dimensionless heat flux $\tilde{q} = q[n\sqrt{2/\pi m}(k_B T_1)^{3/2}]^{-1}$ which is given by

$$\begin{aligned} \tilde{q} = \frac{\sigma_1\sigma_2}{1-(1-\sigma_1)(1-\sigma_2)}\Bigg[\tilde{n}_1\exp(-\tilde{U}_s)\left(1+\frac{1}{2}\tilde{U}_s\right) \\ - \tilde{n}_2\left(\frac{T_2}{T_1}\right)^{3/2}\exp\left(-\tilde{U}_s\frac{T_1}{T_2}\right)\left(1+\frac{1}{2}\tilde{U}_s\frac{T_1}{T_2}\right)\Bigg], \end{aligned} \tag{21}$$

where $\tilde{U}_s = U_s/(k_B T_1)$ and

$$\tilde{n}_1 = 2\Bigg(2\mathrm{erf}(\sqrt{\tilde{U}_s}) + [1-(1-\sigma_1)(1-\sigma_2)]^{-1}\Bigg\{\sigma_1(2-\sigma_2) \times [1-\mathrm{erf}(\sqrt{\tilde{U}_s})] + \sqrt{\frac{T_1}{T_2}}\exp\left[\tilde{U}_s\left(\frac{T_1}{T_2}-1\right)\right] \times \sigma_2(2-\sigma_1)\left[1-\mathrm{erf}\left(\sqrt{\tilde{U}_s\frac{T_1}{T_2}}\right)\right]\Bigg\}\Bigg)^{-1},$$

$$\tilde{n}_2 = \sqrt{\frac{T_1}{T_2}}\exp\left[\tilde{U}_s\left(\frac{T_1}{T_2}-1\right)\right]\tilde{n}_1. \tag{22}$$

As a consistency check, we can compare the expression of Eq. (20) for the case $U_s = 0$ with the literature expression for the free-molecule heat flux. Sparrow and Kinney [10] computed the free-molecular heat flux without force field, but for arbitrary accommodation coefficients at the two surfaces. If $U_s = 0$, Eq. (20) reduces to their equation (up to a constant factor of 4, which is missing in their expression).

III. DISCUSSION AND CONCLUSIONS

To study the effects of the force field and of the boundary conditions separately, we first analyze the case $\sigma_1 = \sigma_2 = 1$. In gas kinetics, accommodation coefficients close to 1 approximate the behavior of many surfaces reasonably well [26,27]. Figure 2 shows the dimensionless heat flux as a function of the temperature ratio T_2/T_1. The curves are labeled with $\tilde{U}_s = U_s/(k_B T_1)$. As expected, the heat flux changes sign with $T_2 - T_1$, being positive for $T_1 > T_2$ and negative for $T_1 < T_2$. For $T_1 < T_2$ the magnitude of the heat flux decreases with increasing $\tilde{U}_s$. In this case the "bottleneck" for heat transfer is the relatively slow particles traveling from surface 1 to surface 2. With increasing $\tilde{U}_s$, fewer and fewer of these particles are able to reach surface 2, and their average kinetic energy decreases. At a value of $\tilde{U}_s = 5$ the heat flux is almost completely suppressed compared to the case without a force field. The situation for $T_1 > T_2$ is more complex. Without a force field it is easy to show that $\tilde{q}$ assumes an absolute maximum at $T_2/T_1 = 1/4$. The reason that the heat flux decreases for $T_2/T_1 < 1/4$ lies in the fact that in the limit

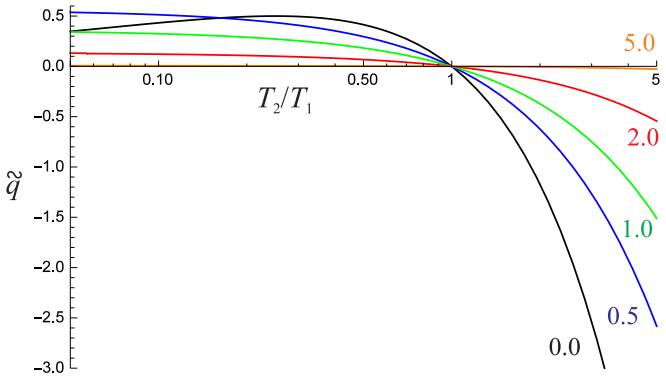

FIG. 2. Dimensionless heat flux as a function of the temperature ratio for the case of diffuse reflection boundary conditions at both surfaces. The curves are labeled with $\tilde{U}_s$.

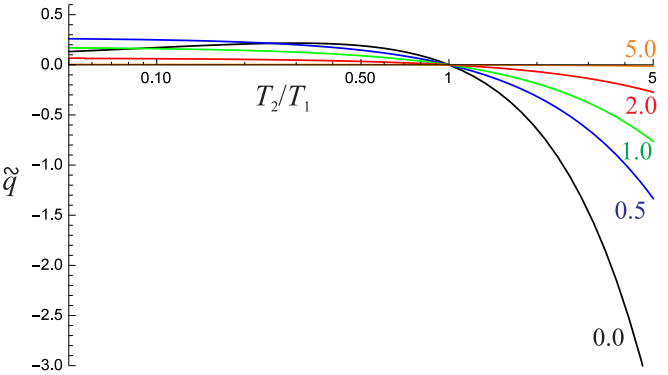

FIG. 3. Dimensionless heat flux as a function of the temperature ratio for $\sigma_1 = 0.5$, $\sigma_2 = 1$. The curves are labeled with $\tilde{U}_s$.

$T_2 \to 0$ the particles leaving surface 2 become so slow that they hardly carry any kinetic energy. At nonzero values of $\tilde{U}_s$ the maximum gets shifted to smaller values of T_2/T_1; in the cases considered in Fig. 2 these values are so small that they fall outside of the range shown on the abscissa. As a consequence, the heat flux at nonzero values of $\tilde{U}_s$ is not always smaller than that obtained for $\tilde{U}_s = 0$, but exceeds the latter if T_2/T_1 is small enough.

Figure 3 shows the heat flux as a function of the temperature ratio for the case $\sigma_1 = 0.5$, $\sigma_2 = 1$. It can be seen that compared to the case with two diffusely reflecting surfaces, the heat flux gets reduced by roughly a factor of 2. For $T_1 \gg T_2$ the heat flux is governed by particles emitted from surface 1. If $\sigma_1 = 0.5$, and based on a statistical interpretation of the surface accommodation coefficient, a surface-particle energy transfer happens in only half of the cases. Likewise, when $T_2 \gg T_1$, the heat transfer is governed by particles emitted from surface 2. If $\sigma_1 = 0.5$, only half of these particles are able to transfer energy to surface 1. Choosing $\sigma_1 = 1$, $\sigma_2 = 0.5$ has roughly the same effect as $\sigma_1 = 0.5$, $\sigma_2 = 1$ (cf. Fig. 4). Only for small values of $\tilde{U}_s$ there is a distinct difference between these two assignments of boundary conditions: $\sigma_1 = 1$, $\sigma_2 = 0.5$ results in a lower (higher) heat flux than $\sigma_1 = 0.5$, $\sigma_2 = 1$ for $T_2 > T_1$ ($T_1 > T_2$).

A force field acting on the particles not only influences the magnitude of the heat flux, it also rectifies the heat flux to a certain degree. Without a force field, replacing T_1 by T_2 at surface

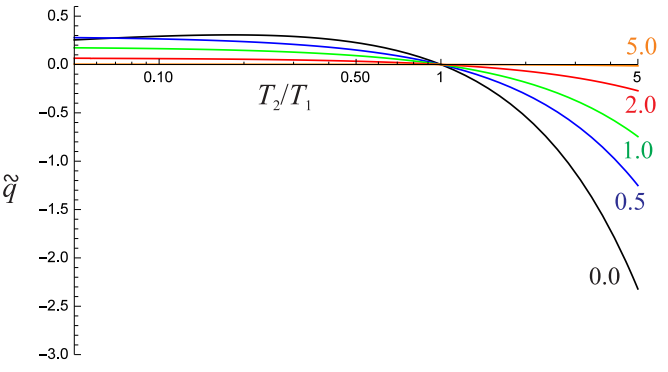

FIG. 4. Dimensionless heat flux as a function of the temperature ratio for $\sigma_1 = 1$, $\sigma_2 = 0.5$. The curves are labeled with $\tilde{U}_s$.

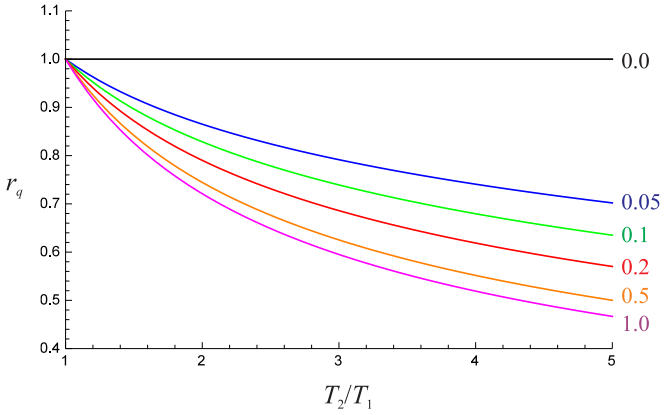

FIG. 5. Heat-flux ratio as a function of the temperature ratio for diffuse reflection boundary conditions at both surfaces. The curves are labeled with $\tilde{U}_s$.

1 and T_2 by T_1 at surface 2 only reverses the sign of the heat flux but does not change its magnitude. By contrast, a thermal diode exhibits a significantly different heat-flux magnitude when the temperatures at its boundary are exchanged. Other than their electronic counterparts, the design of thermal diodes has posed substantial challenges that were difficult to overcome [28,29]. Recently, novel pathways towards thermal rectification have been explored [30–33]. To quantify the thermal rectification, we introduce the heat-flux ratio:

$$r_q = \left|\frac{q(T_1,T_2)}{q(T_2,T_1)}\right| = \left|\frac{\tilde{q}(T_2/T_1)}{\tilde{q}(T_1/T_2)}\right|\left(\frac{T_1}{T_2}\right)^{3/2}. \qquad (23)$$

In Fig. 5 the heat-flux ratio is displayed as a function of T_2/T_1 for diffuse reflection boundary conditions at both surfaces. Since $r_q(T_2/T_1) = 1/r_q(T_1/T_2)$, the values on the abscissa are limited to $T_2/T_1 > 1$. Already a comparatively small $\tilde{U}_s$ of 0.05 gives rise to a significant rectification of the heat flux. The dependence of r_q on $\tilde{U}_s$ is highly nonlinear, such that the deviation from $r_q = 1$ obtained for $\tilde{U}_s = 0.05$ is already more than half of the deviation obtained for $\tilde{U}_s = 1$.

To further shine light on heat-flux rectification, consider a case with disparate values of σ_1 and σ_2. Figure 6 displays the heat-flux ratio as a function of T_2/T_1 for $\sigma_1 = 0.1$, $\sigma_2 = 1$ (top) and $\sigma_1 = 1$, $\sigma_2 = 0.1$ (bottom). The first thing to note is that even at $U_s = 0$ heat-flux rectification occurs. Apparently, the symmetry breaking due to the different assignments of accommodation coefficients at surfaces 1 and 2 is sufficient to induce different heat transport resistances in the two directions.

To explain this heat-flux rectification due to boundary conditions, consider the case $\sigma_1 \ll 1$, $\sigma_2 = 1$, $T_2/T_1 \gg 1$ at vanishing potential. This simple case is constructed to highlight the basic mechanism. To further simplify matters, details of the phase-space distribution will be ignored, and it will be assumed that there are two types of particles, "hot" ones with an energy of the order of $k_B T_2$ and "cold" ones with an energy of the order of $k_B T_1$. If $T_2/T_1 \gg 1$, the contribution to the heat flux by the cold particles can be neglected. To study heat-flux rectification, two different temperature assignments need to be compared, i.e.,

Case A: T_1 at surface 1, T_2 at surface 2;

Case B: T_2 at surface 1, T_2 at surface 2.

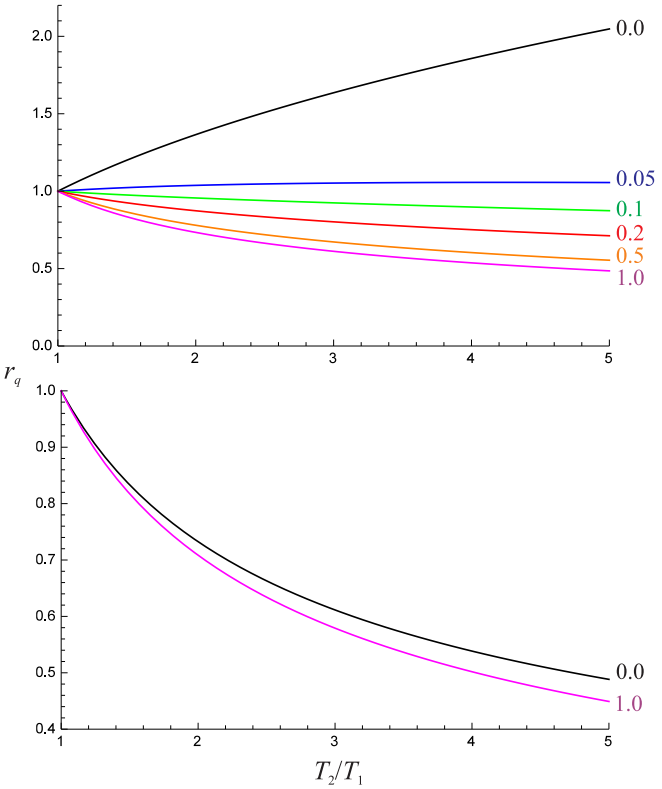

FIG. 6. Heat-flux ratio as a function of the temperature ratio for $\sigma_1 = 0.1$, $\sigma_2 = 1$ (top) and $\sigma_1 = 1$, $\sigma_2 = 0.1$ (bottom). For the latter case, only the curves corresponding to the largest and smallest value of $\tilde{U}_s$ are displayed. The curves representing intermediate values of $\tilde{U}_s$ fall between these two limits.

Under the assumptions made, the magnitude of the heat flux in case A is approximately given by $q_A \sim \sigma_1 N_A k_B T_2$, with N_A being the particle number flux density. This expression is obtained by taking into account that only cold particles impinging at surface 2 contribute to the heat flux (while hot particles impinging at this surface do not, since their kinetic energy is unchanged upon collision with the surface). The probability of a particle hitting surface 2 being cold is given by σ_1, since the conversion of hot into cold particles occurs at surface 1. Likewise, in case B the magnitude of the heat flux is approximately given by $q_B \sim \sigma_1 N_B k_B T_2$, since in this case heat is transferred by hot particles emitted from surface 1. Again, the conversion from cold to hot particles occurs with a probability of σ_1. It is not difficult to see that the particle number flux densities, N_A and N_B, are different. Given that σ_1 is very small, surface 2 determines the kinetic energy of the particles exchanged between the surfaces; i.e., $N_A \sim \sqrt{k_B T_2/m}$, $N_B \sim \sqrt{k_B T_1/m}$. The corresponding heat-flux ratio is obtained as $r_q \sim \sqrt{T_2/T_1}$. Exactly the same expression can be derived from Eq. (20) in the limit $\sigma_1 \to 0$, $T_2/T_1 \to \infty$ (while $\sigma_2 = 1$, $U_s = 0$). This simple example highlights how the boundary conditions cause a heat-flux rectification.

Figure 6 exhibits an interesting influence of the force field on heat-flux rectification. For the case $\sigma_1 = 0.1$, $\sigma_2 = 1$, the rectification is very sensitive to the force field. The substantial rectification occurring at $\tilde{U}_s = 0$ can be virtually eliminated

by applying a comparatively weak potential of $\tilde{U}_s = 0.05$. By contrast, when $\sigma_1 = 1$, $\sigma_2 = 0.1$, the potential has little influence on r_q.

To summarize, the free-molecule heat flux between parallel surfaces was computed analytically in the presence of a conservative force normal to the surfaces. At both surfaces, a Maxwell boundary condition for the reflection of particles was assumed. The force field can give rise to a substantial reduction, but also to an enhancement of the heat flux, depending on the ratio of the temperatures at the two surfaces. Furthermore, the force and/or the boundary conditions for the phase-space distribution function at the two surfaces result in a significant degree of heat-flux rectification. The model developed in this work may be helpful for analyzing various scenarios in which heat is transported ballistically by atoms (or molecules), electrons, or phonons.

[1] C. Cercignani, *Rarefied Gas Dynamics* (Cambridge University Press, Cambridge, 2000).

[2] Y. Sone, *Molecular Gas Dynamics* (Birkhäuser, Boston, 2007).

[3] D. K. Ferry, *Semiconductor Transport* (Taylor & Francis, London, 2000).

[4] C. Jacoboni, *Theory of Electron Transport in Semiconductors* (Springer, Berlin, 2010).

[5] S. Mazumder and A. Majumdar, Monte Carlo study of phonon transport in solid thin films including dispersion and polarization, J. Heat Transfer **123**, 749 (2001).

[6] S. A. Ali, G. Kollu, S. Mazumder, P. Sadayappan, and A. Mittal, Large-scale parallel computation of the phonon Boltzmann transport equation, Int. J. Therm. Sci. **86**, 341 (2014).

[7] C. Shen, *Rarefied Gas Dynamics* (Springer, Berlin, 2005).

[8] J. S. Chawla, X. Y. Zhang, and D. Gall, Effective electron mean free path in TiN(001), J. Appl. Phys. **113**, 063704 (2013).

[9] B. Qiu, Z. Tian, A. Vallabhaneni, B. Liao, J.M. Mendoza, O. D. Restrepo, X. Ruan, and G. Chen, First-principles simulation of electron mean-free-path spectra and thermoelectric properties in silicon, EPL **109**, 57006 (2015).

[10] E. M. Sparrow and R. B. Kinney, Free molecule heat transfer between parallel plates, Phys. Fluids **7**, 473 (1964).

[11] E. P. Gross and S. Ziering, Heat flow between parallel plates, Phys. Fluids **2**, 701 (1959).

[12] J. R. Thomas, T. S. Chang, and C. E. Siewert, Heat transfer between parallel plates with arbitrary surface accommodation, Phys. Fluids **16**, 2116 (1973).

[13] L. Waldmann, Heat transfer through a gas between parallel plates, Z. Naturforsch. A **32**, 914 (1977).

[14] S. K. Loyalka and J. R. Thomas, Heat transfer in a rarefied gas enclosed between parallel plates: Role of boundary conditions, Phys. Fluids **25**, 1162 (1982).

[15] P. J. Clause and M. Mareschal, Heat transfer in a gas between parallel plates: Moment method and molecular dynamics, Phys. Rev. A **38**, 4241 (1988).

[16] C. S. Kim and J. W. Dufty, Heat transport: comparison of theory and simulation, Phys. Rev. A **40**, 6723 (1989).

[17] A. J. Christlieb and W. N. G. Hitchon, Three-dimensional solutions of the Boltzmann equation: Heat transport at long mean free paths, Phys. Rev. E **65**, 056708 (2002).

[18] *Nanoscale Thermoelectrics*, Lecture Notes in Nanoscale Science and Technology Vol. 16, edited by X. Wang and Z. M. Wang (Springer International Publishing Switzerland, Cham, 2014).

[19] E. Macia-Barber, *Thermoelectric Materials* (CRC Press, Boca Raton, FL, 2015).

[20] A. Michaelides and M. Scheffler, An introduction to the theory of crystalline elemental solids and their surfaces, in *Surface and Interface Science*, edited by K. Wandelt (Wiley-VCH, Weinheim, 2014), pp. 13–72.

[21] J. N. Israelachvili, *Intermolecular and Surface Forces*, 3rd ed. (Elsevier, Amsterdam, 2011).

[22] J. A. White, Lennard-Jones as a model for argon and test of extended renormalization group calculations, J. Chem. Phys. **111**, 9352 (1999).

[23] J. A. Barker, R. A. Fisher, and R. O. Watts, Liquid argon: Monte carlo and molecular dynamics calculations, Mol. Phys. **21**, 657 (1971).

[24] S. Daon and E. Pollak, Semiclassical multi-phonon theory for atom-surface scattering: Application to the Cu(111) system, J. Chem. Phys. **142**, 174102 (2015).

[25] A. Bondi, van der Waals volumes and radii, J. Phys. Chem. **68**, 441 (1964).

[26] I. A. Graur, P. Perrier, W. Ghozlani, and J. G. Méolans, Measurements of tangential momentum accommodation coefficient for various gases in plane microchannel, Phys. Fluids **21**, 102004 (2009).

[27] H. Yamaguchi, T. Hanawa, O. Yamamoto, Y. Matsuda, Y. Egami, and T. Niimi, Experimental measurement on tangential momentum accommodation coefficient in a single microtube, Microfluid. Nanofluid. **11**, 57 (2011).

[28] N. A. Roberts and D. G. Walker, A review of thermal rectification observations and models in solid materials, Int. J. Therm. Sci. **50**, 648 (2011).

[29] N. Li, J. Ren, L. Wang, G. Zhang, P. Hänggi, and B. Li, Colloquium: phononics: manipulating heat flow with electronic analogs and beyond, Rev. Mod. Phys. **84**, 1045 (2012).

[30] M. J. Martinez-Perez, A. Fornieri, and F. Giazotto, Rectification of electronic heat current by a hybrid thermal diode, Nat. Nanotechnol. **10**, 303 (2015).

[31] M. Tovar-Padilla, L. Licea-Jimenez, S. A. Pérez-Garcia, and J. Alvarez-Quintana, Enhanced performance thermal diode via thermal boundary resistance at nanoscale, Appl. Phys. Lett. **107**, 084103 (2015).

[32] T. Zhang and T. Luo, Giant thermal rectification from polyethylene nanofiber thermal diodes, Small **11**, 4657 (2015).

[33] Y. Li, X. Shen, Z. Wu, J. Huang, Y. Chen, Y. Ni, and J. Huang, Temperature-dependent transformation thermotics: From switchable thermal cloaks to macroscopic thermal diodes, Phys. Rev. Lett. **115**, 195503 (2015).